Nanosilica supported CaO: A regenerable and mechanically hard CO_2 sorbent at Ca-looping conditions

P. E. Sanchez-Jimenez[a], L. A. Perez-Maqueda[a], J. M. Valverde[b*],

[a] Instituto de Ciencia de Materiales (C.S.I.C.-Univ. Seville) Americo Vespucio 49, 41092 Sevilla, Spain.

[b] Faculty of Physics. University of Seville. Avenida Reina Mercedes s/n, 41012 Sevilla, Spain

(Dated: November 29, 2013)

Abstract

This work presents a CO_2 sorbent that may be synthesized from low-cost and widely available materials following a simple method basically consisting of impregnation of a nanostructured silica support with a saturated solution of calcium nitrate. In a first impregnation stage, the use of a stoichiometric CaO/SiO_2 ratio serves to produce a calcium silicate matrix after calcination. This calcium silicate matrix acts as a thermally stable and mechanically hard support for CaO deposited on it by further impregnation. The CaO-impregnated sorbent exhibits a stable CaO conversion at Ca-looping conditions whose value depends on the CaO wt% deposited on the calcium silicate matrix, which can be increased by successive reimpregnations. A 10wt%CaO impregnated sorbent reaches a stable conversion above 0.6 whereas the stable conversion of a 30wt%CaO impregnated sorbent is around 0.3, which is much larger than the residual conversion of CaO derived from natural limestone (between 0.07 and 0.08). Moreover, particle size distribution measurements of samples predispersed in a liquid and subjected to high energy ultrasonic waves indicate that the CaO-impregnated sorbent has a relatively high mechanical strength as compared to limestone derived CaO.

* **Corresponding author at:** Department of Electronics and Electromagnetism, Faculty of Physics, Avda. Reina Mercedes s/n, 41012 Seville (Spain). Phone no. +34 954550960. Fax no. +34 954239434. Email: jmillan@us.es

I. INTRODUCTION

Calcium-looping (CaL) technology is emerging as a viable CO_2 capture process based on the carbonation reaction of CaO at high temperature and the subsequent calcination of $CaCO_3$ to regenerate the sorbent [1–3]. The process has recently been investigated for its implementation in diverse industrial applications such as postcombustion CO_2 capture [4], enhancement of steam methane reforming via precombustion CO_2 capture [5], and storage of thermal energy [6, 7]. Postcombustion CO_2 capture by means of the CaL technology received the highest R&D priority from the Technology Task Force of the European Technology Platform for ZeroEmission Power Plants [8]. Capture efficiencies over 90% have been achieved in pilot-scale plants of up to 1.7 Mw_{th} [9], which raises hopes of scaling up the CaL technology to commercial demonstrations in the near future. In regards to the so-called sorption enhanced steam methane reforming (SE-SMR) process, higher methane to hydrogen conversion and improved energy efficiency are achieved by in-situ capture of CO_2 while steam methane reforming and water gas shift reactions are taking place [5, 10]. Commercially available gasification technologies have been integrated with the CO_2 sorption-enhanced watergas shift process for advanced coal-based power plants showing a satisfactory performance [11]. Moreover, a concentrated solar power (CSP) plant concept has been proposed which uses the CaL technology for heat transport and storage [7]. Concentrated solar energy is applied to the calciner providing the energy required for decarbonation whereas energy is released and transferred into the carrying air to a gas turbine from the exothermic carbonation between CaO and stored CO_2.

While the most suitable material and operating parameters for an optimum performance of SE-SMR and CaL-CSP industrial plants are a subject of current research [7], they appear to be well defined for CO_2 postcombustion capture [2]. In the practical application, CaO particles must react in a fluidized bed reactor (carbonator) with the CO_2 present at low concentrations (around 15% vol) in an inlet stream of flue gas flowing at velocities of a few m/s. After a short residence time the partially carbonated particles are circulated into a second fluidized bed reactor (calciner) to liberate by calcination the captured CO_2 as a pure stream ready for transportation and storage. By taking into account the tradeoff between the reaction equilibrium driving force and its kinetics, carbonation/calcination are carried out at temperatures of around 650°C/900°C, respectively. Concerning the material

to be employed as CaO precursor, low cost and widely available natural limestone seems to standout as the best practical choice for industrial applications [12].

Thermogravimetric analysis (TGA) experiments demonstrate that carbonation of limestone derived CaO particles proceeds along two well differentiated phases. After a first kinetically-controlled fast reaction phase on the surface of the solid follows a much slower reaction, which is controlled by solid-state diffusion of CO_2 through the solid. The fast carbonation stage is ended when a carbonate layer (30-50 nm thick [13]) is developed on the particle's surface. In practice, CaO conversion is limited by short residence times and low CO_2 partial pressure, which mainly constrains it to the fast carbonation phase [14]. Thus, CaO conversion in the CaL technology is critically affected by the sorbent surface area available for fast carbonation, which is progressively reduced by calcination as the number of cycles builds up [13, 15]. As a consequence, fast CaO conversion suffers a particularly marked sharp drop in the first carbonation/calcination cycles converging towards a stable residual value after a large number of cycles of just about 0.07 - 0.08 for natural limestones [16]. Thus, in order to achieve a sustainable capture efficiency, high solids recirculation rates must be imposed while poorly active sorbent is periodically replaced by fresh limestone [14]. This brings about significant operating challenges whereas an excessive amount of fresh makeup limestone hampers the thermal efficiency of the process [2, 3, 17]. Enhancing the conversion stability of CaO-based sorbents is thus a current challenge to improve the efficiency of the CaL technology.

An active direction of research aimed at the achievement of high and stable CaO conversion at Ca-looping conditions is the modification/synthesis of Ca-based sorbents [18, 19]. In this work we analyze the use of silica as a reliable and widely available low-cost material whose use has been already proposed in several works to attenuate the decay of multicyclic CaO conversion. Cheap precursors such as rice husks (of high SiO_2 content) can be used to produce low-cost high purity and high surface area nanosilica by means of simple processes [20–22]. Chen at al. [23] have studied the performance of a synthetic sorbent prepared by mixing rice husk ash with CaO in an aqueous solution. Wu et al. [24] used a sol-gel method to synthesize a nanostructured synthetic sorbent consisting of nano-$CaCO_3$ particles with an amorphous SiO_2 film. Huang et al. [25] synthesized a composite sorbent from a wet mixture of calcium acetate hydrate and a mesoporous silica molecular sieve SBA-15, which served as a stable framework for CaO to inhibit its deactivation. In a previous work

we have shown that CaO conversion is enhanced for a nanosilica/CaO composite derived from calcination of a nanosilica/$Ca(OH)_2$ dry mixture [26, 27]. Diverse applications have also benefited from the thermal stability provided by nanosilica. Thus, nanosilica has been proposed as a thermally stable support of CO_2-absorbents polyethoxyamine fluids [28] and as additive of molten salts to promote their thermal properties [29]. In a recently reported study, nanosilica derived from rice husks has been employed as a support for catalysts following an impregnation method, which provides the supported catalyst with a high activity and regenerability [30]. In this paper, we analyze the performance of a synthetic CO_2 sorbent at CaL conditions obtained from impregnation of calcium nitrate on a nanosilica support. The synthetic sorbent is shown to exhibit a stable conversion well above the residual conversion of natural limestones. Furthermore, Particle Size Distribution (PSD) measurements of samples subjected to high energy ultrasonic waves capable of producing particle fragmentation demonstrate that the mechanical strength of the CaO-impregnated sorbent is enhanced as compared to CaO derived from natural limestone.

II. MATERIAL PREPARATION AND CHARACTERIZATION

Calcium nitrate tetrahydrate ($Ca(NO_3)_2{\cdot}4H_2O$ from Sigma-Aldrich) and a nanostructured silica powder (commercially available Aerosil® 300 from Evonik) have been used is our work as primary materials. Aerosil®300 is a hydrophilic and amorphous fumed silica (Fig. 1) derived from flame hydrolysis with a reported BET surface area of 300±30 m^2/g [31]. Silica nanoparticles are seen to be structured in aggregates of size between tens to hundreds of microns [32]. Even though high purity starting reagents have been employed in our lab-scale research, cheaper alternatives can be found for its potential use in larger scale settings. Low-cost calcium nitrate (commonly found as a tetrahydrate due to air moisture absorption) is in fact employed in a number of large-scale commercial applications. Low-cost nanosilica may be produced by means of simple processes involving cheap precursors (such as rice husks) and is also used in industrial applications as, for example, in the production of concrete mixtures with high compressive strength [21, 33]. For comparison, a high purity natural limestone (99.62wt% $CaCO_3$, 0.24wt% MgO, 0.08wt% Na_2O, SiO_2 <0.05wt%, Al_2O_3 <0.05wt%) supplied to us by Segura S.L. (Matagallar quarry, Pedrera, Spain) will be used in our study.

For preparation, a sample of previously dried nanosilica was impregnated with a saturated aqueous solution of calcium nitrate tetrahydrate by means of the incipient wetness impregnation technique (also called capillary impregnation or dry impregnation), which is a commonly used technique for the synthesis of heterogeneous catalysts [34]. During the impregnation process the $Ca(NO_3)_2{\cdot}4H_2O$ solution is drawn into the pores of the nanosilica support. Later on the mixture is heated up to 650°C in air. $Ca(NO_3)_2{\cdot}4H_2O$ melts at 43°C. Above the boiling point at 135°C water is progressively lost until dehydration is completed at about 200°C [35]. $Ca(NO_3)_2$ melts at 560°C and subsequent decomposition ($2\ Ca(NO_3)_2 \rightarrow 2\ CaO + 4\ NO_2 + O_2$) occurs in the molten phase [36]. After decomposition, the material was calcined at 900°C. X-ray analysis indicates that CaO reacts with SiO_2 upon calcination to form calcium silicate ($2CaO + SiO_2 \rightarrow Ca_2SiO_4$). In a first impregnation stage, the amount of calcium nitrate to be impregnated on the SiO_2 support was calculated as to balance the CaO/SiO_2 stoichiometric ratio for formation of calcium silicate. In this first stage, a calcium silicate matrix was thus obtained as the only byproduct as may be seen in the XRD pattern shown in Fig. 2 where only peaks corresponding to Ca_2SiO_4 are distinguishable (sample identified as 0wt% CaO). Multicyclic carbonation/calcination tests (carried out as detailed in the next section) showed that this sample does not have an appreciable CO_2 capture capacity at the CaL conditions employed in our TGA tests close to the Ca-looping conditions. Further reimpregnations were thus carried out on this Ca_2SiO_4 matrix, which served to coat it with increasing amounts of CaO. TEM images and selected-area electron diffraction (SAED) analysis (Fig. 3) show that the CaO supported on the calcium silicate matrix has a crystalline structure. XRD patterns obtained for diverse impregnated sorbents are plotted in Fig. 2 for 10, 23, 30, and 40wt% CaO-impregnated sorbents (wt% of CaO calculated from the mass of nitrate used for reimpregnation). In accordance with the increasing load of CaO built up on the silicate matrix by successive reimpregnations, the intensity of the CaO peaks in the XRD patterns is increased whereas the silicate peaks intensity remain practically unchanged (Fig. 2). In contact with ambient air, the samples suffered a certain degree of carbonation (peaks of low intensity corresponding to $CaCO_3$ may be seen in some XRD patterns), which was however negligible if the time period between preparation and testing was short (less than a few hours).

SEM micrographs illustrate that the surface texture of the decomposed calcium nitrate on its own (Fig. 4a) is markedly changed when decomposed on the calcium silicate support

(Fig. 4b). Higher magnification SEM pictures are illustrated in Fig. 6 showing a uniform layering of CaO on the calcium silicate support. Energy-Dispersive X-ray (EDX) spectra (Fig. 4d) derived from diverse selected areas indicate accordingly that Ca is evenly distributed on the surface of the impregnated sorbent. Since calcium nitrate decomposes in the molten state, the formation of pores is impaired as it progresses to CaO. Accordingly, SEM pictures are indicative of a low porosity sorbent as compared to CaO derived from limestone calcination (Fig. 6). A characteristic feature inferred from our SEM analysis is the development of bottleneck CaO bridges between the impregnated grains resulting from calcium nitrate decomposition in the molten state on the silicate matrix (see Fig. 6). A similar phenomenon has been observed in other materials synthesized by impregnation [37].

Figure 4c shows the pore size distributions obtained for decomposed calcium nitrate on its own (BET=0.5 m^2/g), and a 20wt%CaO impregnated sorbent (BET=3 m^2/g). Pore size distributions of limestone (BET=0.8 m^2/g) and CaO (BET=6.2 m^2/g) derived from limestone decarbonation (850°C in air for 30 min) are also plotted for comparison. As may be seen, the pore population of decomposed calcium nitrate on its own is rather small and pores smaller than 6 nm are undetectable. The carbonation performance at CaL conditions of CaO derived from calcium nitrate decomposition on its own has been previously investigated by Lu et al. [38] who showed that it has a very low CO_2 capture capacity due to its extremely small porosity upon decomposition as confirmed in our study. In contrast, decomposition of limestone yields a relatively large population of small pores in the range 2-6 nm left behind by CO_2. This provides the resulting CaO skeleton with a high reactivity in a first carbonation as early noted by Barker [15]. On the other hand, even though the porosity of the CaO-impregnated sorbent is increased as compared to that of calcium nitrate decomposed on its own, Fig. 4c shows that the population of small pores remains low. The CaO-impregnated sorbent exhibits however a similar pore distribution to that of CaO derived from limestone in the region of larger pores ($> 8nm$). In regards to the effect of increasing the CaO wt% by successive reimpregnations, Fig. 5 illustrates a gradual reduction of the impregnated sorbent porosity as the CaO wt% is increased as might have been expected.

III. EXPERIMENTAL RESULTS AND DISCUSSION

A. Multicyclic CaO conversion

Multicyclic CaO conversion tests have been performed by means of a Q5000IR TG analyzer (TA Instruments). This equipment is provided with an infrared halogen furnace and with a high sensitivity balance (<0.1 μg) characterized by a minimum baseline dynamic drift (<10 μg). The use of an infrared halogen furnace in our TGA runs allowed us for heating/cooling the sample very quickly (up to 500°/min for linear heating range) overcoming the problem of slow heating rates typically employed in conventional TGA instruments (of about 50°C min^{-1} or even smaller [39]) that lead to excessively long transitional periods far from Ca-looping conditions in practice.

Prior to carbonation/calcination cycles, the sample (around 10 mg) is calcined in-situ in the TG analyzer by increasing the temperature up to 850°C in dry air following a linear heating ramp (20°C/min), which leads to decarbonation if the sample had suffered partial carbonation between preparation and the test. Once the material is preheated, the temperature is decreased down to 650°C (cooling rate 300°C/min) and the sorbent is subjected to a flow (100 $cm^3 min^{-1}$) of a dry gas mixture (85% air/15% CO_2 vol/vol) for carbonation to proceed during 5 minutes. Next, the calcination stage of the cycle is carried out by heating the sorbent up to 850°C (heating rate 300°C/min) for 5 minutes in a dry air flow. After calcination, the temperature is again decreased to continue with the carbonation stage of a new cycle.

Figure 7 shows data on the multicyclic CaO conversion (ratio of grams of CaO converted to CaO initial) measured for impregnated sorbents and for natural limestone. As may be observed, conversion of limestone derived CaO in the 1st carbonation reaches a high level ($X_1 \simeq 0.74$) as expected from the relatively large population of small pores upon quick decomposition by preheating. Yet, a steep drop of conversion is seen in the next cycles as widely documented in the literature [1]. After 50 cycles, a conversion is reached already close to the residual value measured for natural limestones in a wide variety of conditions ($X_r \simeq 0.07 - 0.08$) [16]. On the other hand, the sorbent impregnated with a 40wt% CaO has a practically stable conversion of about 0.15 from the 1st cycle. As seen in Fig. 7a, a reduction of the CaO wt% below 40% gives rise to a multicyclic behavior characterized by

reactivation. The small activity exhibited by the impregnated sorbents in the 1st carbonation can be explained from its low porosity as inferred from physisorption measurements. After the 1st carbonation, the decomposition of the carbonated layer by calcination would yield a porous CaO skeleton which would be prone to sinter during the rest of the calcination stage. However, the observed reactivation suggests that the Ca_2SiO_4 matrix serves to hinder an excessive sintering of this nascent CaO skeleton thus preventing the decay of conversion with the cycle number as typically featured by limestone. Arguably, the stabilizing effect of the Ca_2SiO_4 matrix would be more noticeable as the CaO wt% is decreased. Thus, the porosity of the nascent CaO skeleton (regenerated upon decomposition of the carbonate layer in each cycle) might increase progressively with the cycle number as sintering is more efficiently precluded by the thermally stable support. Conversion is therefore seen to increase with the cycle number until a stable value is reached after about 25 cycles which is close to 0.3 for a CaO wt% between 20 and 30% and is above 0.6 for the 10wt% CaO-impregnated sorbent. Even though the activity of these impregnated sorbents is small in the first cycle, a suitable strategy to increase it would consist of carbonating them before the multicyclic tests are carried out. This is seen in Fig. 7b, where results are shown for an impregnated sorbent preheated in-situ in a 15%CO_2/85%air gas mixture (vol/vol) causing partial carbonation and rapid decomposition before the start of carbonation/calcination cycles. In this way the initial CaO skeleton (partly derived from decomposition of $CaCO_3$) is provided with a higher porosity, which leads to a higher conversion in the 1st cycle. Likewise, if the impregnated sorbent is carbonated just by leaving it exposed to ambient air for a long period of time its conversion in the first cycle is seen to be increased up to a value comparable to that of limestone (Fig. 7b). Note that, even though the initial activity of these carbonated sorbents is relatively high, it decays with the cycle number converging to a stable value, which is independent of the pretreatment. This stable residual value would be thus only determined by the stabilizing effect of the silicate support, which is a function of the CaO wt% built up on it by reimpregnation.

It is worth noting that the sorbents analyzed in our study have been subjected to mild calcination conditions for regeneration in the multicyclic tests. On other hand, complete decarbonation of limestone in short times under the CO_2 rich atmosphere of the calciner would require application of temperatures above 900°C [1, 40] that would enhance CaO sintering [40, 41]. A recent analysis [42] on the decarbonation kinetics of partially carbonated

particles (∼15% $CaCO_3$ as typical for the solids exiting the carbonator) has revealed that, according to practical constraints such as high CO_2 partial pressure in the calciner (50 - 70 kPa) and short residence times (2 - 3 min) [43], the calcination temperature can be lowered down to 870 - 880°C. Expectedly, the enhanced thermal stability of the impregnated sorbents would serve to preserve a high CaO conversion even at high calcination temperatures as opposed to the drastic drop of conversion observed for limestone derived CaO due to enhanced sintering at severe calcination conditions [1, 40].

B. Mechanical strength of the impregnated sorbent

Besides the progressive loss of activity of natural limestone derived CaO, a major issue that besets the CaL technology is that calcined limestone is a rather mechanically fragile material, which leads to high particle attrition rates and sorbent losses by elutriation [1, 40]. On the other hand, it is well known that the use of nanosilica as additive is a successful strategy to enhance the compressive strength and abrasion resistance of high performance cement-based materials [21, 33]. In this section we will analyze whether the sorbent synthesized in our work using nanosilica is also provided with an enhanced mechanical strength. To this end particle size distributions of CaO samples have been measured using a Mastersizer 2000 instrument (Malvern Instruments), which measures particle size by means of laser diffractometry of a predispersed sample. Usually, predispersion is carried out in this instrument in-situ by subjecting the dry powder to a high-velocity air jet before the sample is driven into the measuring cell. Figure 8a shows the particle size distribution (PSD averaged on three independent tests showing low variability) of CaO derived from limestone calcination and predispersed using an air dispersive pressure of 0.1 bar, which generates air jet velocities of around 10 m/s [44]. As may be seen, large particles resisting mechanical impacts in the predispersion unit can be still detected in the measuring cell. Alternatively, sample predispersion may be carried out prior to PSDs measurements in a liquid, which is a more convenient method if only small amounts of material are available for testing as for the CaO-impregnated sorbent synthesized in our study. The wet sample predispersion unit employed in our work was the Hydro 2000S, which comprises an electric motor that drives a stirrer and impeller in the dispersion tank to provide a simultaneous stirring and pumping action that moves the agitated sample via the sample tubing to the cell located in the optical

bench. In our work, a synthetic sorbent sample (2.5 g) was dispersed in 2-propanol (100 ml). This concentration has been chosen as recommended by the international standard for laser diffraction measurements ISO 14887. According also to this standard, 2-propanol has been selected as a suitable dispersant for Ca-based particles to ensure the solid not to be dissolved or chemically react with the liquid. The PSD obtained for the CaO-impregnated sorbent is shown in Fig. 8b.

Measuring the PSD of samples predispersed in a liquid and subjected to high energy ultrasonic irradiation may be useful to infer information on the mechanical strength of the solids [45]. Intense acoustic waves cause fragmentation of solid particles by their interaction with collapsing cavities in the liquid [46]. Fragmentation of $CaCO_3$ particles suspended in a liquid and subjected to high energy ultrasonic irradiation has been recently observed in-situ by high speed photography [47]. Figure 8 shows the PSDs of limestone derived CaO and CaO-impregnated sorbent samples predispersed in 2-propanol and subjected to ultrasonic irradiation (150 W, 40 kHz for 10 min). Since laser diffraction is a volume-based technique, the dynamic range covered is quite broad (between 0.02 and 2000 μm), which allows detecting big particles as well as fine fragments resulting from attrition [48]. As may be seen in Fig. 8, high energy ultrasonic irradiation causes an extensive generation of fine fragments for limestone derived CaO (the average particle size is decreased from 56 μm down to 4 μm), which is consistent with the markedly fragmentation pattern generally reported for calcined limestones subjected to high impact loading and conforming to a disintegration failure mode [49]. In the case of the CaO-impregnated sorbent, ultrasonic irradiation yields also a reduction of particle size but to a lesser extent (the average particle size is decreased from 82 μm down to 32 μm). Fracture of brittle materials is due to the presence of randomly distributed flaws or cracks in the solid [50, 51]. The strength of a given particle is thus determined by the weakest flaws/crack and depends on the particle size. Assuming that flaws/cracks are randomly distributed on the solid with a constant density per unit volume, their number is expected to increase as particle size is increased. Thus, the energy required to fracture a particle is generally a decreasing function of particle size [50, 51]. Taking into account the larger average size of the particles in the CaO-impregnated sorbent as compared to limestone derived CaO particles as well as the significantly smaller degree of particle size reduction by ultrasonic irradiation, it may be concluded that the CaO-impregnated sorbent particles have a relatively higher resistance to fragmentation. Arguably, strong chemical

bonds due to the formation of calcium silicate as well as the physical nanostructure of the silica matrix would be responsible for providing the sorbent with an enhanced mechanical strength, which would bring about an added benefit to the use of this synthetic sorbent in the CaL technology.

IV. CONCLUSIONS

In this study a synthetic CO_2 sorbent is presented which may be obtained from low-cost and widely available materials and is prepared by a simple process based on incipient wetness impregnation technique. In a first stage of the preparation process, a nanostructured silica matrix is impregnated with a saturated solution of calcium nitrate at the stoichiometric ratio necessary to produce calcium silicate after calcination. In a second stage, the calcium silicate matrix is further reimpregnated. Decomposition of calcium nitrate in the molten state yields an evenly distributed CaO layer on the thermally stable calcium silicate matrix. As a result, sintering of CaO in the calcination stage of the carbonation/calcination cycles is hindered. In contrast with the drastic decay of (limestone derived) CaO conversion with the number of carbonation/calcination cycles, the conversion of the impregnated sorbent either remains stable or is increased with the cycle number reaching a high residual value that depends on the CaO wt%. For a CaO wt% between 20 and 30%, the residual conversion is close to 0.3, which is well above the residual conversion of natural limestone derived CaO (between 0.07 and 0.08). High values of initial conversion comparable to that of limestone derived CaO may be achieved by precarbonating the impregnated sorbent. In this case the calcium silicate matrix mitigates the rate of conversion decay with the cycle number converging towards a stable value similar to that of impregnated samples not subjected to precarbonation. Besides of the improved thermal stability, the impregnated sorbent is provided with a high mechanical strength as inferred from measurements of the particle size distribution of samples predispersed in a liquid and subjected to high energy ultrasonic irradiation. These measurements indicate a relatively high resistance to attrition of the CaO-impregnated particles as compared to natural limestone derived CaO for which ultrasonic irradiation generates a considerable population of fine particles caused by fragmentation.

V. ACKNOWLEDGEMENTS

This work was supported by the Andalusian Regional Government (Junta de Andalucia, contract FQM-5735) and Spanish Government Agency Ministerio de Ciencia e Innovacion (contracts FIS2011-25161 and CTQ2011-27626). We gratefully acknowledge the Microscopy, Functional Characterization, and X-ray services of the Innovation, Technology and Research Center of the University of Seville (CITIUS) as well as Drs. M.A.S. Quintanilla and J. Perez Vaquero for his help with the PSD measurements.

---

[1] J. Blamey, E. J. Anthony, J. Wang, and P. S. Fennell, "The calcium looping cycle for large-scale CO_2 capture," *Prog. Energ. Combust. Sci.*, vol. 36, no. 2, pp. 260–279, 2010.

[2] M. C. Romano, "Modeling the carbonator of a Ca-looping process for CO_2 capture from power plant flue gas," *Chemical Engineering Science*, vol. 69, pp. 257 – 269, 2012.

[3] P. Lisbona, A. Martinez, and L. M. Romeo, "Hydrodynamical model and experimental results of a calcium looping cycle for CO_2 capture," *Applied Energy*, vol. 101, pp. 317 – 322, 2013.

[4] A. Sanchez-Biezma, J. Ballesteros, L. Diaz, E. de Zarraga, F. Alvarez, J. Lopez, B. Arias, G. Grasa, and J. Abanades, "Postcombustion CO_2 capture with CaO. status of the technology and next steps towards large scale demonstration," *Energy Procedia*, vol. 4, no. 0, pp. 852 – 859, 2011.

[5] M. C. Romano, E. N. Cassotti, P. Chiesa, J. Meyerb, and J. Mastin, "Application of the sorption enhanced-steam reforming process in combined cycle-based power plants," *Energy Procedia*, vol. 4, pp. 1125–1132, 2011.

[6] J. M. Criado, M. Macias, and A. Macias-Machin, "Analysis of the system CaO-CO_2-H_2O for storage of solar thermal energy," *Solar Energy*, vol. 49, pp. 83–86, 1992.

[7] S. E. Edwards and V. Materic, "Calcium looping in solar power generation plants," *Solar Energy*, vol. 86, no. 9, pp. 2494 – 2503, 2012.

[8] Zero Emmissions Plataform Task Force on Technology, *Recommendations for RTD, Support Actions and International Collaboration activities within FP7 Energy Work Programmes and National RTD Programmes in support of deployment of CCS in Europe.* European Technology Platform for Zero Emission Fossil Fuel Power Plants, April 2008.

[9] B. Arias, M. Diego, J. Abanades, M. Lorenzo, L. Diaz, D. Martinez, J. Alvarez, and A. Sanchez-Biezma, "Demonstration of steady state {CO_2} capture in a 1.7 MWth calcium looping pilot," *International Journal of Greenhouse Gas Control*, vol. 18, pp. 237 – 245, 2013.

[10] K. Johnsen, H. J. Ryu, J. R. Grace, and C. J. Lim, "Sorption-enhanced steam reforming of methane in a fluidized bed reactor with dolomite as CO_2-acceptor," *Chem. Eng. Sci.*, vol. 61, no. 4, pp. 1195–1202, 2006.

[11] S. Chen, W. Xiang, D. Wang, and Z. Xue, "Incorporating IGCC and CaO sorption - enhanced process for power generation with CO_2 capture," *Applied Energy*, vol. 95, pp. 285 – 294, 2012.

[12] N. Rodriguez, M. Alonso, J. C. Abanades, A. Charitos, C. Hawthorne, G. Scheffknecht, D. Y. Lu, and E. J. Anthony, "Comparison of experimental results from three dual fluidized bed test facilities capturing CO_2 with CaO," *Energy Procedia*, vol. 4, pp. 393 – 401, 2011.

[13] G. Grasa, R. Murillo, M. Alonso, and J. C. Abanades, "Application of the random pore model to the carbonation cyclic reaction," *AIChE J.*, vol. 55, no. 5, pp. 1246–1255, 2009.

[14] J. C. Abanades, E. J. Anthony, D. Y. Lu, C. Salvador, and D. Alvarez, "Capture of CO_2 from combustion gases in a fluidized bed of CaO," *AIChE J.*, vol. 50, no. 7, pp. 1614–1622, 2004.

[15] R. Barker, "Reversibility of the reaction $CaCO_3$ =CaO+CO_2," *J. Appl. Chem. Biotechnol.*, vol. 23, pp. 733 – 742, 1973.

[16] G. S. Grasa and J. C. Abanades, "CO_2 capture capacity of CaO in long series of carbonation/calcination cycles," *Ind. Eng. Chem. Res.*, vol. 45, no. 26, pp. 8846–8851, 2006.

[17] B. Arias, J. C. Abanades, and G. S. Grasa, "An analysis of the effect of carbonation conditions on CaO deactivation curves," *Chem. Eng. J.*, vol. 167, no. 1, pp. 255–261, 2011.

[18] W. Liu, H. An, C. Qin, J. Yin, G. Wang, B. Feng, and M. Xu, "Performance enhancement of calcium oxide sorbents for cyclic CO_2 capturea review," *Energy & Fuels*, vol. 26, no. 5, pp. 2751–2767, 2012.

[19] J. M. Valverde, "Ca-based synthetic materials with enhanced CO_2 capture efficiency," *J. Mater. Chem. A.*, vol. 1, p. 447 468, 2013.

[20] C. Real, M. D. Alcala, and J. M. Criado, "Preparation of silica from rice husks," *J. Am. Ceram. Soc.*, vol. 8, p. 2012 2016, 1996.

[21] N. Thuadaij and A. Nuntiya, "Synthesis and characterization of nanosilica from rice husk ash prepared by precipitation method," *CMU. J. Nat. Sci. Special Issue on Nanotechnology*, vol. 7, p. 59 65, 2008.

[22] K. Amutha, R. Ravibaskar, and G. Sivakumar, "Extraction, synthesis and characterization of nanosilica from rice husk ash," *International Journal of Nanotechnology and Applications*, vol. 4, p. 61 66, 2010.

[23] H. Chen, C. Zhao, and Q. Ren, "Feasibility of CO_2/SO2 uptake enhancement of calcined limestone modified with rice husk ash during pressurized carbonation," *Journal of Environmental Management*, vol. 93, no. 1, pp. 235 – 244, 2012.

[24] R. Wu and S. Wu, "Performance of nano-$CaCO_3$ coated with SiO_2 on CO_2 adsorption at high temperature," *Huagong Xuebao (Chinese Edition)*, vol. 57, pp. 1722 – 1726, 2006.

[25] C.-H. Huang, K.-P. Chang, C.-T. Yu, P.-C. Chiang, and C.-F. Wang, "Development of high-temperature CO_2 sorbents made of cao-based mesoporous silica," *Chemical Engineering Journal*, vol. 161, no. 12, pp. 129 – 135, 2010.

[26] J. M. Valverde, A. Perejon, and L. Perez-Maqueda, "Enhancement of fast CO_2 capture by a nano-SiO_2/CaO composite at Ca-looping conditions," *Environmental Science & Technology*, vol. 46, no. 11, pp. 6401 – 6408, 2012.

[27] J. M. Valverde, P. E. Sanchez-Jimenez, A. Perejon, and L. A. Perez-Maqueda, "Constant rate thermal analysis for enhancing the long-term CO_2 capture of CaO at ca-looping conditions," *Applied Energy*, vol. 108, pp. 108 – 120, 2013.

[28] O. M. Al-Azzawi, C. M. Hofmann, G. A. Baker, and S. N. Baker, "Nanosilica-supported polyethoxyamines as low-cost, reversible carbon dioxide sorbents," *Journal of Colloid and Interface Science*, vol. 385, p. 154 159, 2012.

[29] D. Shin and D. Banerjee, "Enhanced specific heat capacity of nanomaterials synthesized by dispersing silica nanoparticles in eutectic mixtures," *J. Heat Transfer*, vol. 135, p. 032801(1) 032801(8), 2013.

[30] E. Rafiee and S. Shahebrahimi, "Nano silica with high surface area from rice husk as a support for 12-tungstophosphoric acid: An efficient nano catalyst in some organic reactions," *Chin. J. Catal.*, vol. 33, p. 1326 1333, 2012.

[31] http://www.aerosil.com/product/aerosil/en/products/hydrophobic-fumed silica/pages/default.aspx, "Product information," tech. rep., Evonik Degussa GmbH, 2011.

[32] M. A. S. Quintanilla, J. M. Valverde, M. J. Espin, and A. Castellanos, "Electrofluidization of silica nanoparticle agglomerates," *Ind. Eng. Chem. Res.*, vol. 51, pp. 531 – 538, 2012.

[33] K. Sobolev, I. Flores, L. M. Torres-Martinez, P. Valdez, E. Zarazua, and E. L. Cuellar, "Engineering of SiO_2 nanoparticles for optimal performance in nano cement-based materials," in *Nanotechnology in Construction 3* (J. Nemecek, Z. Bittnar, P. J. M. Bartos, Z. Bittnar, P. J. M. Bartos, V. Smilauer, and J. Zeman, eds.), pp. 139 – 148, Springer Berlin Heidelberg, 2009.

[34] J. Regalbuto, *Catalyst Preparation: Science and Engineering*. CRC Press, 2007.

[35] J. Paulik, F. Paulik, and M. Arnold, "Thermogravimetric examination of the dehydration of calcium nitrate tetrahydrate under quasiisothermal and quasi-isobaric conditions," *Journal of thermal analysis*, vol. 27, no. 2, pp. 409–418, 1983.

[36] C. Ettarh and A. K. Galwey, "A kinetic and mechanistic study of the thermal decomposition of calcium nitrate," *Thermochimica Acta*, vol. 288, no. 1-2, pp. 203 – 219, 1996.

[37] J. Wang, L. Li, W. Liu, Y. Wang, Y. Wang, and M. Zhou, "Sc_2O_3 – W matrix impregnated cathode with spherical grains," *Journal of Physics and Chemistry of Solids*, vol. 69, no. 8, pp. 2103 – 2108, 2008.

[38] H. Lu, E. P. Reddy, and P. G. Smirniotis, "Calcium oxide based sorbents for capture of carbon dioxide at high temperatures," *Ind. Eng. Chem. Res.*, vol. 45, pp. 3944 – 3949, 2006.

[39] D. Y. Lu, R. W. Hughes, E. J. Anthony, and V. Manovic, "Sintering and reactivity of $CaCO_3$-based sorbents for in situ CO_2 capture in fluidized beds under realistic calcination conditions," *J. Environ. Eng.*, vol. 135, no. 6, pp. 404–410, 2009.

[40] V. Manovic, J.-P. Charland, J. Blamey, P. S. Fennell, D. Y. Lu, and E. J. Anthony, "Influence of calcination conditions on carrying capacity of CaO-based sorbent in CO_2 looping cycles," *Fuel*, vol. 88, pp. 1893–1900, 2009.

[41] J. M. Valverde, P. E. Sanchez Jimenez, A. Perejon, and L. A. Perez-Maqueda, "CO2 multicyclic capture of pretreated/doped CaO in the ca-looping process. theory and experiments," *Phys. Chem. Chem. Phys.*, vol. 15, pp. 11775 – 11793, 2013.

[42] I. Martinez, G. Grasa, R. Murillo, B. Arias, and J. C. Abanades, "Kinetics of calcination of partially carbonated particles in a ca-looping system for CO_2 capture," *Energy & Fuels*, vol. 26, no. 2, pp. 1432 – 1440, 2012.

[43] I. Martinez, R. Murillo, G. Grasa, and J. Carlos Abanades, "Integration of a Ca looping system for CO2 capture in existing power plants," *AIChE Journal*, vol. 57, no. 9, pp. 2599–2607, 2011.

[44] F. Ecker, N. Mueller, and D. Nikolai, "Comparative studies of various methods for determining the friability of granules and the development of a quick test by laser diffraction," in *DPhG Jahrestagung*, (September 29th – October 1st, Jena, Germany), pp. –, 2009.

[45] J. M. Valverde and M. A. S. Quintanilla, "Attrition of ca-based co_2-adsorbents by a high velocity gas jet," *AIChE Journal*, vol. 59, no. 4, pp. 1096–1107, 2013.

[46] K. A. Kusters, S. E. Pratsinis, S. G. Thoma, and D. M. Smith, "Ultrasonic fragmentation of agglomerate powders," *Chem. Eng. Sci.*, vol. 48, no. 24, pp. 4119–4127, 1993.

[47] R. Wagterveld, L. Boels, and M. M. G. Witkamp, "Visualization of acoustic cavitation effects on suspended calcite crystals," *Ultrasonics Sonochemistry*, vol. 18, no. 1, pp. 216 – 225, 2011.

[48] M. Instruments, "Detecting oversized particles in ceramic powders using the mastersizer 2000," application note, Malvern Instruments, 2005.

[49] F. Scala, F. Montagnaro, and P. Salatino, "Attrition of limestone by impact loading in fluidized beds," *Energy & Fuels*, vol. 21, pp. 2566–2572, 2007.

[50] S. Yashima, Y. Kanda, and S. Sano, "Relationships between particle size and fracture energy or impact velocity required to fracture as estimated from single particle crushing," *Powder Technol.*, vol. 51, no. 3, pp. 277–282, 1987.

[51] P. M. Amaral, J. C. Fernandes, and L. G. Rosa, "Weibull statistical analysis of granite bending strength," *Rock Mech. Rock Engng.*, vol. 41, pp. 917–928, 2008.

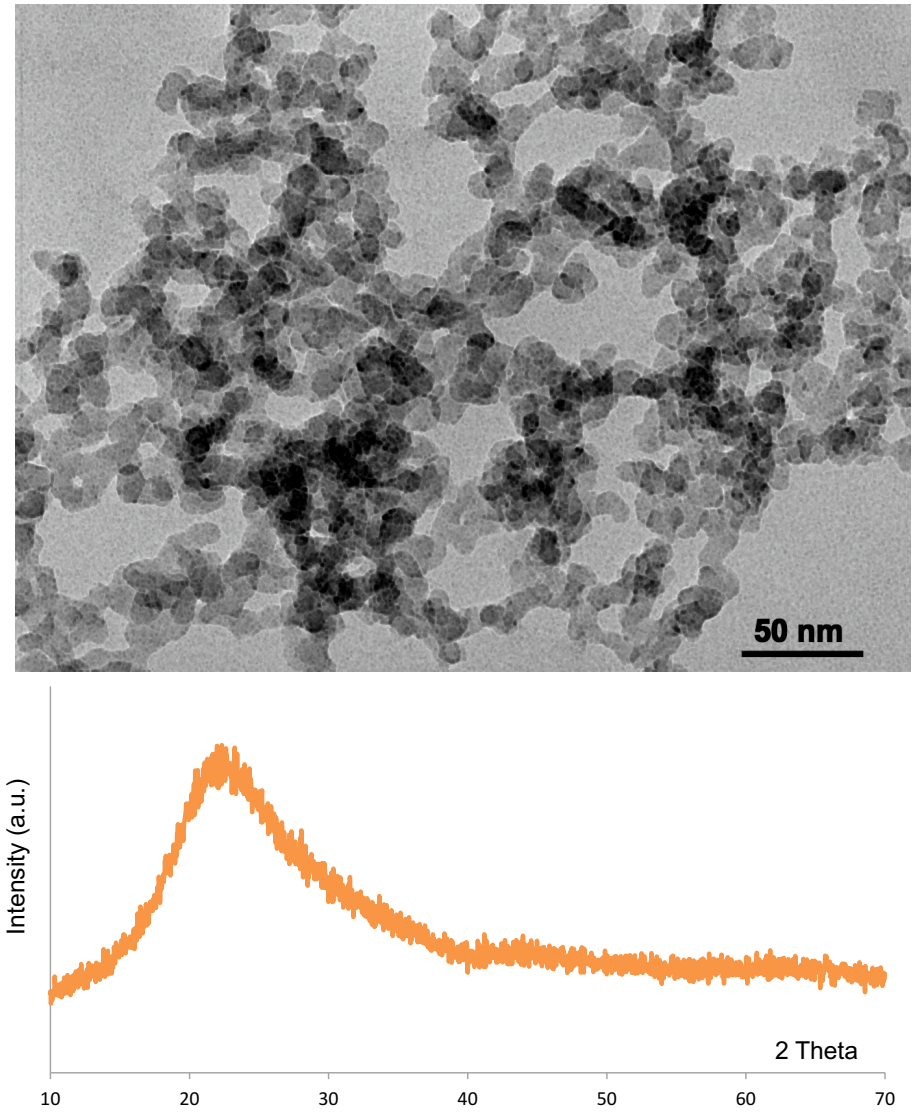

FIG. 1. TEM micrograph (Philips CM200 microscope) of the fumed nanosilica powder used in this work and XRD diagram demonstrating a characteristic amorphous structure.

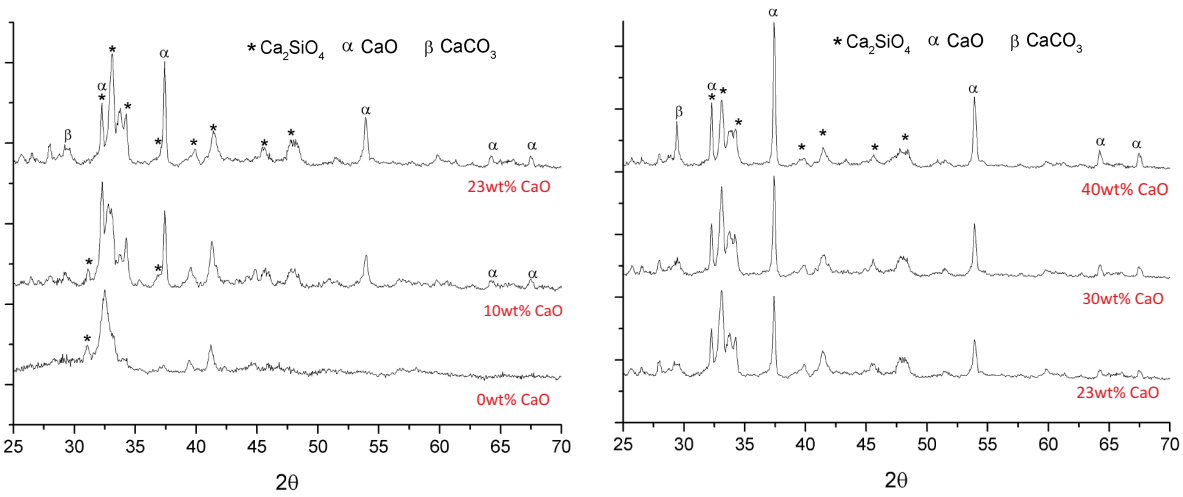

FIG. 2. XRD patterns of sorbent samples obtained just after being synthesized by impregnation of calcium nitrate onto a nanosilica matrix. The 0 wt% CaO case corresponds to a sample prepared using the stoichiometric CaO/SiO_2 ratio to yield only calcium silicate. The wt% of CaO indicated in the other cases corresponds to the weight percentage of CaO built up in excess on the calcium silicate support after subsequent impregnations.

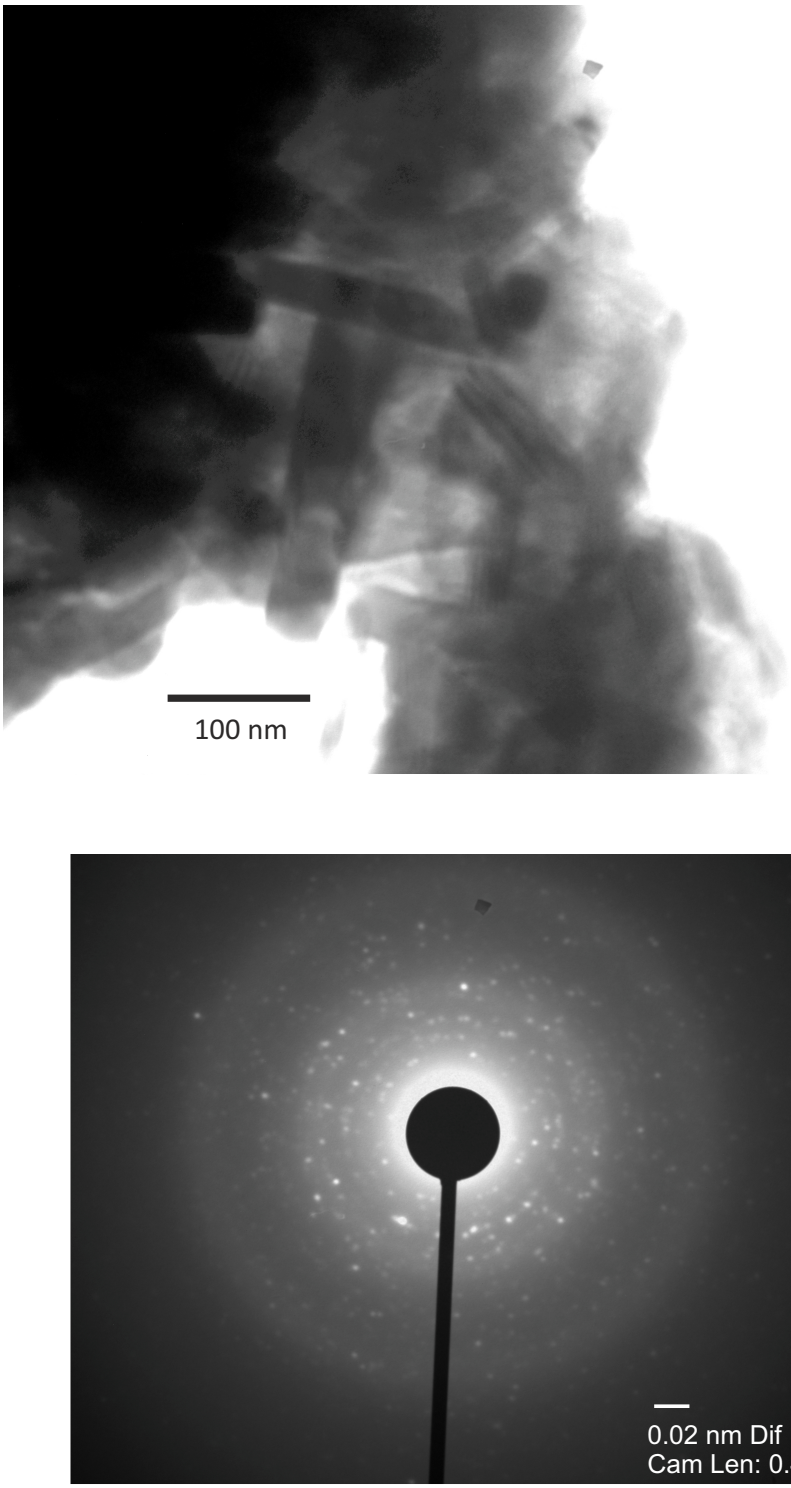

FIG. 3. TEM image and electron diffraction pattern of the 20wt%CaO-impregnated sorbent. Obtained using a H800 Philips microscope.

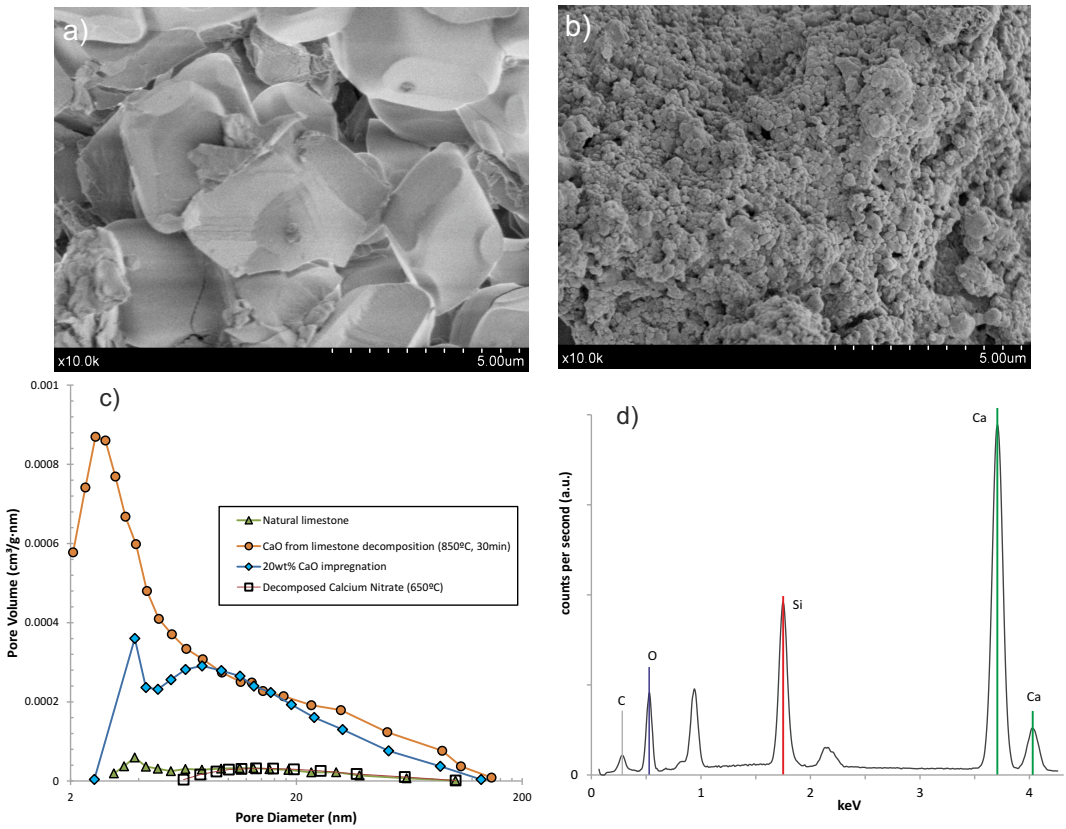

FIG. 4. SEM pictures of decomposed calcium nitrate on its own (a) and decomposed calcium nitrate after impregnation on the calcium silicate matrix (b, 20%wt CaO). c) BJH desorption (dV/dD) pore volume distributions for decomposed calcium nitrate on its own, impregnated sorbent, limestone and CaO from limestone decarbonation. d) Example of Energy Dispersive Spectroscopy (EDX) analysis of the impregnated sorbent showing Si, Ca, C and O corresponding to calcium carbonate and calcium silicate (the other peaks correspond to Cu present in the supporting grid). SEM/EDX obtained using a Hitachi S520 microscope. Porosity analysis obtained using a TriStar II 3020 V1.03 analyzer operated by N_2 adsorption at 77 K.

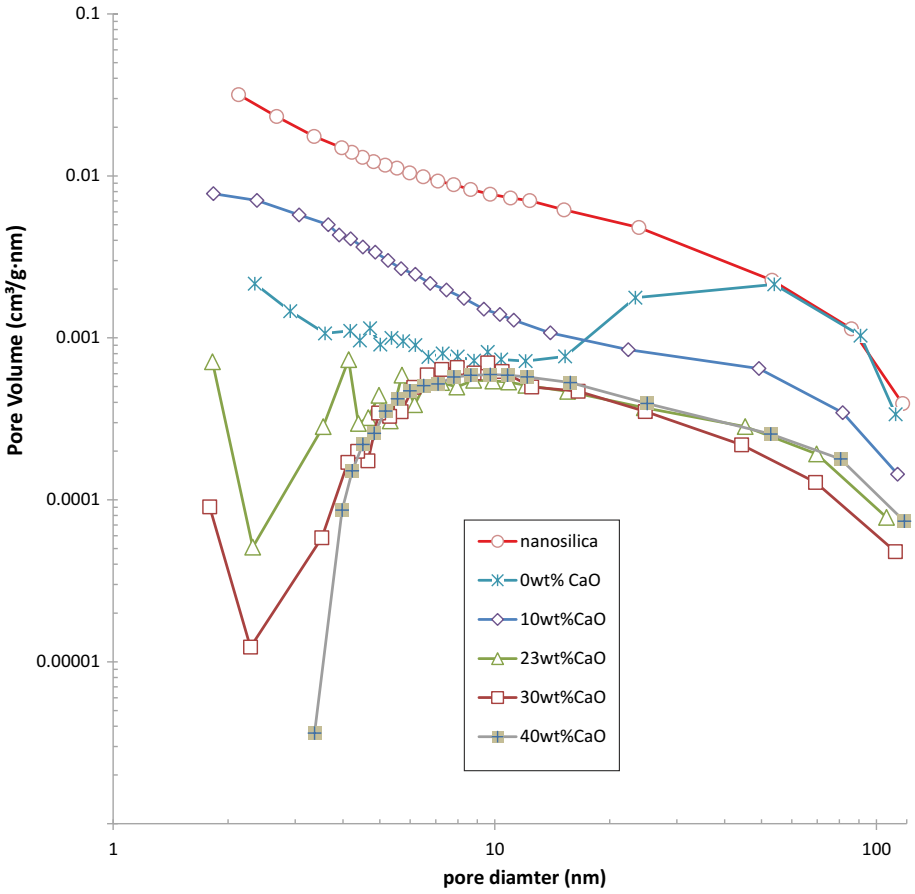

FIG. 5. BJH desorption (dV/dD) pore volume distributions for nanosilica and impregnated sorbents. The 0 wt% CaO case corresponds to a sample prepared using the stoichiometric CaO/SiO_2 ratio to yield only calcium silicate. The wt% of CaO indicated in the other cases corresponds to the weight percentage of CaO built up in excess on the calcium silicate support after subsequent impregnations.

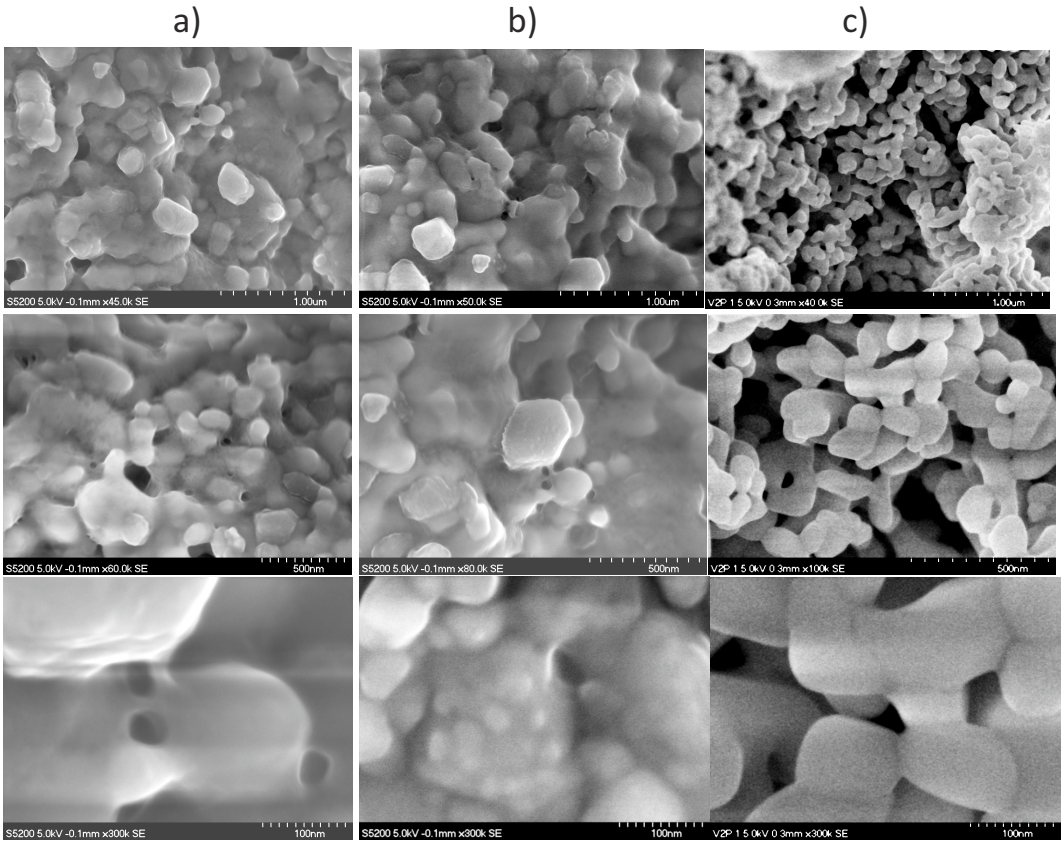

FIG. 6. High magnification SEM pictures of the 20wt%CaO-impregnated sorbent (a and b) and calcined limestone (c). Obtained using a Hitachi S520 microscope.

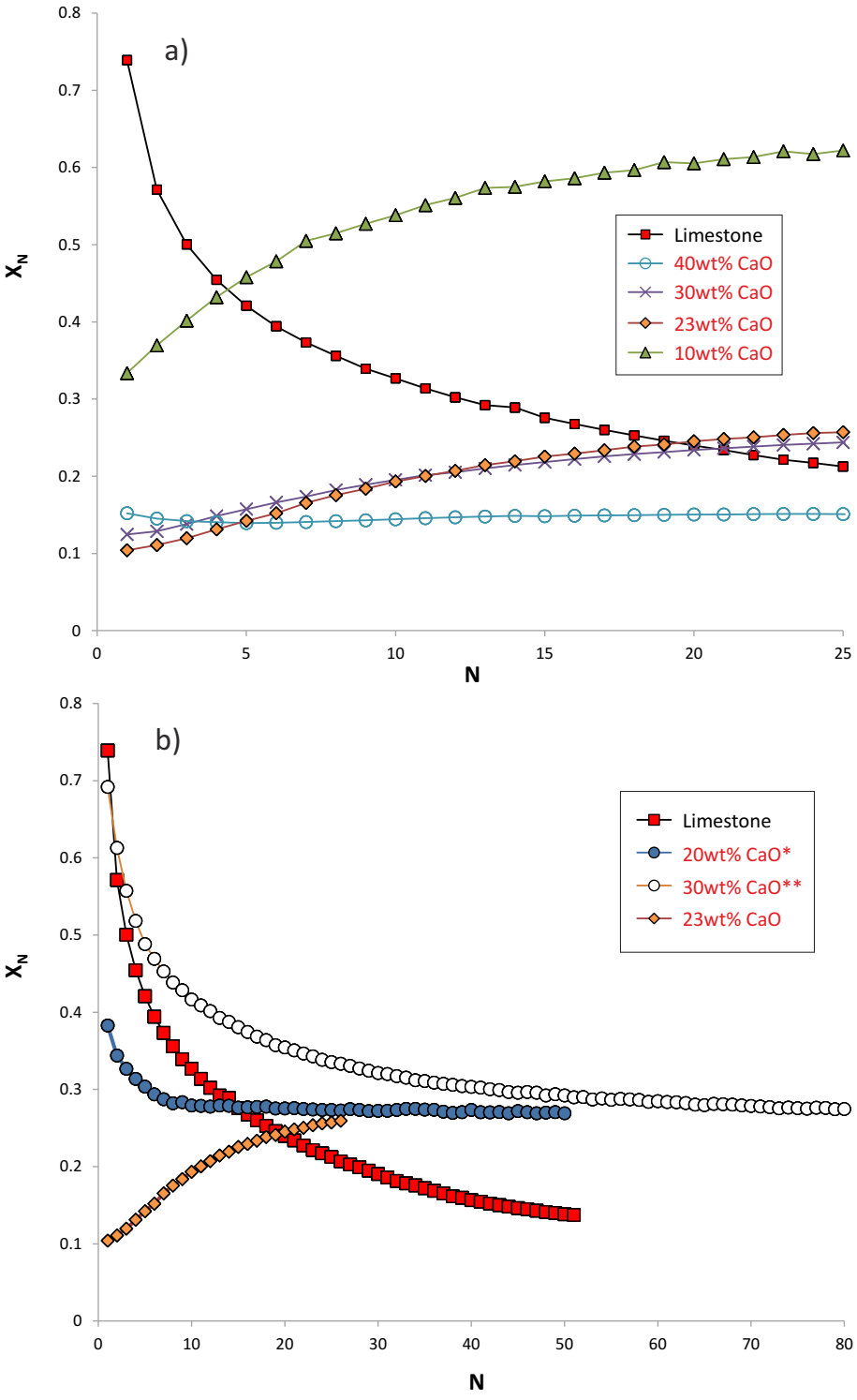

FIG. 7. d) CaO conversion at the end of the 5 min carbonation stage vs. cycle number for the impregnated sorbents (10, 23, 30, and 40wt%CaO) and for natural limestone. Figure b shows results obtained for samples impregnated and thereafter carbonated. 20wt% CaO* is carbonated in-situ by linear preheating in a 15%CO_2/85% air gas mixture. 30wt% CaO*∗ is carbonated by leaving it exposed to ambient air for several weeks.

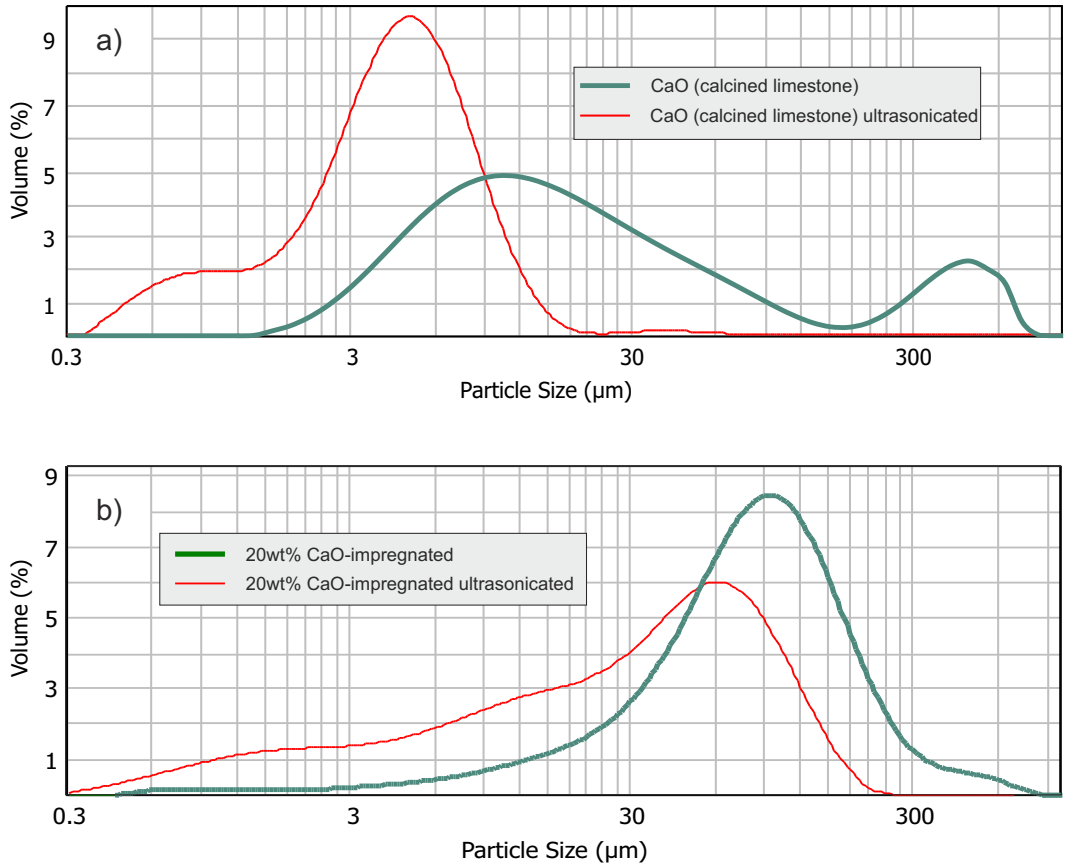

FIG. 8. a) PSDs obtained by laser diffractometry of samples of calcined limestone (dispersed in-situ by a 0.1 bar air jet) and predispersed in 2-propanol where it is subjected to high energy ultrasonic irradiation. b) PSDs of samples of 20wt%CaO-impregnated sorbent (calcined as a final step of its preparation) predispersed in 2-propanol (non subjected and subjected to ultrasonic irradiation).